

## INTERFEROMETRIC STUDIES OF THE BRAZILIAN CUÍÇA

Tatiana Statsenko, Vasileios Chatziioannou, Wilfried Kausel

Institute of Music Acoustics  
University of Music and Performing Arts Vienna, Austria  
statsenko@mdw.ac.at

### ABSTRACT

Electronic speckle pattern interferometry (ESPI) has been implemented for investigation of the vibrational behavior of the Brazilian *cuíça*. An advanced filtering and processing of time-averaging ESPI data has been applied to a friction drum, which has not been studied by means of laser interferometry before. Asymmetry in the operating deflection shapes of the *cuíça* has been observed and discussed. The obtained results were compared to finite element method computer simulations and single-point laser Doppler vibrometer deformation measurements. Vibrational shapes of the *cuíça* occurring under harmonic excitation are presented along with corresponding simulated mode shapes followed by the discussion of irregular patterns. The results of ESPI show an agreement with simulations and provide quantitative data on absolute values of the deformation amplitude.

### 1. INTRODUCTION

Drums are generally played by striking with hands or sticks. However, some percussion instruments, such as the *cuíça*, the lion's roar and the *buhai*, are excited by friction, which is applied on a wooden stick or a string, attached to the center of a membrane which is stretched on one open end of a cylindrical body. The playing principle of friction drums can be compared to violin bowing as it involves the stick-slip process which occurs when one object is sliding relative to another. This comprises continuous and transient actions, resulting in a complex and nonlinear response [1]. However, at low excitation amplitudes it is possible to describe the operating deflection shapes of the membrane with relation to normal modes, whereas at large amplitude they may show distinctly nonlinear or chaotic behavior.

The acoustical properties of the *cuíça* have been covered in a limited number of works and require more advanced examination, which can be given by non-contact optical methods, such as electronic speckle pattern interferometry (ESPI) and laser Doppler vibrometry (LDV), widely used in non-destructive investigation of vibrating objects [2]. Both techniques have been applied to musical instruments [3–6] and show high agreement with theoretical predictions on modal shapes, allowing full-field contactless measurements without special preparation of instruments. LDV uses the Doppler effect of a shifted frequency which occurs when light is reflected from the moving object. ESPI is an interferometric technique based on coherence properties of light diffracted from a rough surface. Microscopic variations in surface height produce scattered light in all directions and, due to high coherence of the laser, the amplitudes of the waves sum up. Imaging results in a granular pattern with spatial distribution of the intensity which solely depends on the diffraction limit of the camera [7]. Though speckles carry information

on object movement, they reduce image quality and create 'salt and pepper' noise, so the main challenge is to retrieve the deformation phase change, which is highly affected by random phase distribution.

Time-averaging ESPI has evolved from holographic interferometry and provides fast and quantitative analysis on vibrations and small displacements of the whole object. It is a well-known optical method for non-contact deformation analysis with a conventional camera and a low-power continuous laser, which makes acquisition easy and does not require any specific conditions [7, 8]. The term "time-averaging" comes from the capturing procedure, since the acquisition time of a conventional detector is much higher than the period of vibration of the object under investigation.

The principal aim of this study was to investigate the vibration modes of a nonlinear friction drum under harmonic excitation with a simple low-cost experimental setup based on time-averaging speckle interferometry and supplemented with extensional advanced data processing.

### 2. CUÍÇA

The *cuíça* is a Brazilian friction drum, brought from Africa and widely used in samba music as a rhythm and solo instrument [9]. The modern *cuíça*, shown in Figure 1, is made of an aluminum tube with ribs and a single drumhead made of animal skin.



Figure 1: Modern *cuíça*, produced by Meinl Percussion. The photo is taken from the manufacturer's website.

The body can be also made of a gourd (folk *cuíça*), wood or fiberglass. A thin bamboo stick is bound to the center of the membrane, and the sound is produced by gentle rubbing of the stick with a piece of damp cloth in one hand, while the other hand alters the pitch by pressing against the center of the drum. If the second hand is not touching the drumhead, this results in an open tone [10]. In the sitting position the drum is horizontally placed on a knee of a performer, while for standing it is held at chest height, carried with a strap. The *cuíça* produces a high pitched sound recalling an animal voice with large dynamic range.

In the present paper, a 15 cm diameter cuíca drum from Meinl Percussion is investigated. The membrane is made of goat skin, approximately 0.3 mm thick. Harmonic excitation at low amplitudes does not reflect real playing conditions, yet it helps to visualize mode shapes and avoid excessive nonlinearities.

### 3. TIME-AVERAGING ESPI

Among various experimental techniques of ESPI, a reference-updating method was chosen because of its simplicity in implementation and higher intensity contrast compared to classical time-averaging interferometry [11]. An induced linear decorrelation of speckle phases between frames is introduced and subsequent images are being subtracted, revealing correlation fringes, which express levels of equal displacement of the object between two captures. This subtraction procedure eliminates decorrelation noise which generally occurs when the time between two compared frames increases. The output images can be displayed on the screen in real time and the shape of correlation fringes gives information about operating deflection shapes of the object at different frequencies.

#### 3.1. Theory

Consider two interfering coherent light beams with spatially random phases, and a phase difference  $\phi_0$ . One beam is reflected from an object, and another one is a reference beam originating from the same source. Due to the imaging system both beams are speckled and, in order to simplify the equations, a single pixel index is assumed. Assuming a linear phase shift in the reference beam and the external excitation of the object, the phase variation  $\phi$  due to harmonic motion at frequency  $\omega_0$  can be temporally described as:

$$\phi(t) = \phi_0 + \gamma t + \xi \sin(\omega_0 t), \quad (1)$$

where  $\gamma$  is a coefficient directly linked to the velocity of the object due to the introduced linear movement and  $\xi$  describes harmonic motion and contains information about the vibration amplitude of the object  $A$ :

$$\xi = \frac{4\pi A}{\lambda}, \quad (2)$$

where  $\lambda$  is the wavelength of light. The time-averaged intensity of the  $n$ -th frame in a series of images measured by the detector is [11]:

$$\langle I_n \rangle = I_O + I_R + \beta \langle \cos(\phi_n + \gamma t + \xi \sin \omega_0 t) \rangle, \quad (3)$$

where  $I_O$  and  $I_R$  are intensities of two interfering beams,  $\beta$  is intensity modulation, and  $\phi_n$  is a random phase defined for every pixel. It is assumed that if the time between two consecutive exposures is relatively short, the random phase changes only due to the linear shift. When two subsequent images taken during vibration are being subtracted, the resulting output intensity is:

$$I_{\text{sub}}(\xi) = \beta \left| \frac{1}{t_{\text{exp}}} \int_0^{t_{\text{exp}}} \cos[\phi_n + \gamma(t_{\text{cam}} + t) + \xi \sin \omega_0 t] dt - \frac{1}{t_{\text{exp}}} \int_0^{t_{\text{exp}}} \cos[\phi_n + \gamma t + \xi \sin \omega_0 t] dt \right|. \quad (4)$$

Generally, the exposure time  $t_{\text{exp}}$  and the time between two captures  $t_{\text{cam}}$  are not equivalent, so they are distinguished from

each other. Equation (4) does not have a general analytic solution. However, it can be approximated by:

$$I_{\text{sub}}(\xi) = |\mu \beta J_0(\xi)|, \quad (5)$$

where the coefficient  $\mu$  depends only on parameters given by the linear movement and camera characteristics:

$$\mu = \frac{4}{\gamma t_{\text{exp}}} \left| \sin\left(\frac{\gamma}{2} t_{\text{cam}}\right) \sin\left(\frac{\gamma}{2} t_{\text{exp}}\right) \sin\left(\frac{\gamma}{2} (t_{\text{exp}} + t_{\text{cam}}) + \phi_n\right) \right|. \quad (6)$$

The random phase  $\phi_n$  immensely affects intensity and overall image quality. Low-pass filtering does not solve the problem, since it reduces fringe contrast. However, there are other ways to improve the images. The speckle size is given by the illumination wavelength and camera characteristics which can be adjusted so that each pixel accumulates several speckles. Image quality can be further enhanced by the averaging of several images, since the averaging of  $n$  frames decreases the speckle noise  $\sqrt{n}$  times [12].

Therefore, nodes corresponding to  $\xi = 0$  give maximum output intensity and are easily detected in an ESPI picture. Moving parts are defined by correlation fringes, given by Equation (5), with peak values rapidly decreasing as amplitude increases. However, phase and deformation amplitude values cannot be easily retrieved by taking the inverse of  $|J_0(\xi)|$ . The Bessel function is quasi-periodic, so the resulting phase map would be “wrapped” over a single interval from zero to the first root of the Bessel function. In phase-shifting ESPI the phase unwrapping procedure to obtain full-field data consists of adding integral multiples of  $2\pi$  to the phase, preserving spatial continuity of the surface [13]. In reference-updating ESPI, regional inversion of the Bessel function, involving detection of minimum and maximum levels of the intensity within each side lobe region, is more appropriate due to different peak levels of the side lobes.

The proposed phase retrieving algorithm consists of enumeration of isolated contours and an order assignment of the corresponding side lobes of the Bessel function. For each area, maximum values are found and unwrapped. Contours of black correlation fringes are converted to phase data in the same fashion. First order regions can be processed on a pixel base, giving higher spatial resolution. The process assumes continuity of the object and provides no ambiguity of the side lobe order detection. Higher precision is achieved through pixel-by-pixel inversion based on retrieved data, but needs more computational time. The resulting absolute phase values can be easily converted to deflection amplitudes, providing quantitative data on vibration amplitude for every pixel.

#### 3.2. Experimental setup

Consider the setup shown in Figure 2. Light from a laser source is split in two beams, one serving as an object illumination and a second being a reference beam. A mirror, mounted on a piezoelectric transducer (PZT), is introduced in the reference arm and provides an adjustable temporal optical path difference. A ground glass placed on the path of the reference beam serves as a diffuser which generates a scattered field and facilitates the alignment procedure. The two beams are combined upon the surface of the camera, therefore the average speckle size of both beams is the same. Rotation of polarizers controls the intensity of both beams. A continuous wave 532 nm laser operated at a power of 0.2 W. The frame rate of the camera was 11 fps for a resolution of  $2050 \times 2448$  pixels.

The cuíca was fixed on the same table as all optical elements, and the bamboo stick was sinusoidally excited by a

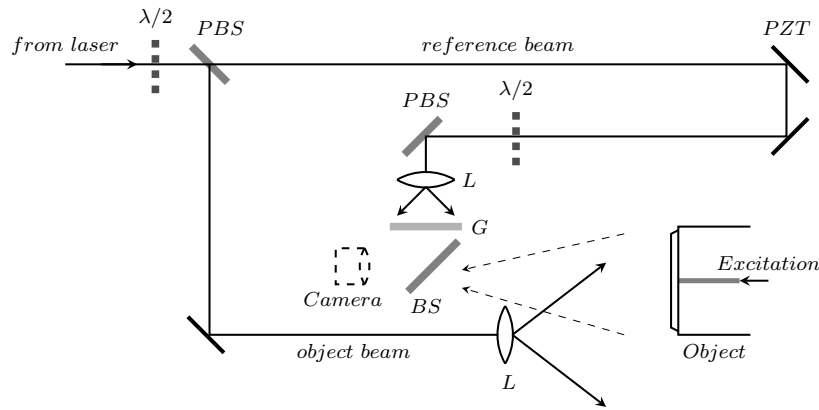


Figure 2: Setup for an ESPI measurement. Light from the laser is divided into two beams by a polarizing beamsplitter (*PBS*). Both beams are expanded by lenses (*L*). Half-wave plates ( $\lambda/2$ ) are added to control the relative intensity of the beams. A reference beam is passing through the ground glass (*G*), and then the two beams are combined by a beamsplitter (*BS*) and directed to the camera. A PZT-mirror adds a linear phase shift during image capturing.

shaker mounted behind the instrument so that the only moving parts of the instrument were the stick and the membrane. The amplitude and frequency of the shaker were controlled by a frequency generator. The contrast of ESPI images was adjusted by changing the relative intensity of the beams, the amplitude of the PZT and the number of frames recorded during each cycle of the PZT. The image capturing and the PZT driving were done using LabVIEW software.

#### 4. RESULTS

Along with experiments, the normal modes of the cuíca were studied using the finite element method (FEM) implemented in COMSOL Multiphysics. The investigation was done for a pre-tensioned membrane with a radius of 75 mm, clamped along the borders. Harmonic excitation was applied to a circular area of 5 mm in diameter, shifted by 1.4 mm from the center. The parameters used for the simulation of the membrane are shown in Table 1. They were chosen from analogous membrane materials and adjusted while comparing the model to the experimental values [14, 15].

Parameter	Value
Pre-tension	4470 N/m
Young's modulus	50 MPa
Density	1260 kg/m <sup>3</sup>
Poisson's ratio	0.3

Table 1: Parameters for COMSOL modeling.

##### 4.1. ESPI

Analysis has been done for excitation frequencies from 200 Hz to 2000 Hz. An unwrapping procedure was preceded by averaging, normalization and digital filtering of sequences of frames, all performed in MATLAB. Series of images were averaged in order to decrease speckle noise. The procedure of normalization involved division by the averaged reference frame, taken without any external excitation. Normalization removed undesirable diffraction effects and artifacts caused by dust. Spatial filtering was followed by localized Fourier transform filtering

(LFF), based on the method described by Li [16]. The difference from LFF is that there is no Gaussian smoothing, and filtering is performed on the inverted images which positively affects the output contrast. The results of phase unwrapping for three vibrational states of the cuíca are presented in Figure 3 together with FEM simulations.

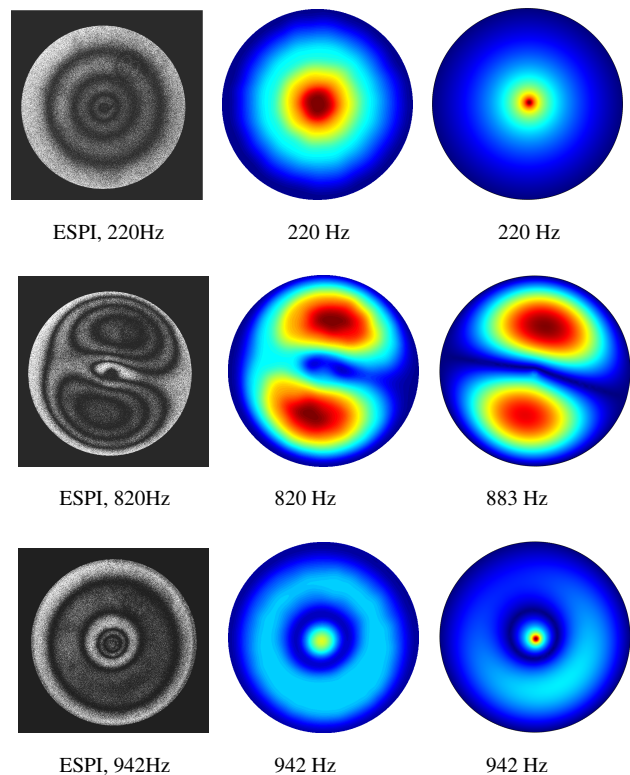


Figure 3: Unwrapping of two ESPI patterns and comparison to FEM predictions. Left: temporally averaged ESPI images. Middle: unwrapped data. Right: corresponding simulations.

The simulation was performed for exact experimental values of the frequencies where it was possible, but for certain values there was a discrepancy between experimental data and corresponding normal modes. Therefore, the closest solutions have been chosen. The wooden stick is connected not to the exact

center of the membrane, which causes asymmetry of the operating deflection shapes. This asymmetry may also be reinforced by inhomogeneity of the membrane and a slight tilt of the bamboo stick which changes the vector of the applied force. Thus, operating deflection shapes which imply only circular nodes become highly asymmetric with increasing excitation force. Such an example is shown in Figure 4 for the vibration amplitude at 872 Hz. The same result can be achieved for a totally symmetric object, when an additional component of the direction of applied force is introduced in the plane of the membrane. Such a small variation in location and direction of the applied force drastically changes the deformation shape of the membrane. Regarding the real tension of the membrane, it cannot be easily modeled. Since goat skin is not perfectly homogeneous, it changes along its area randomly. Simple altering of the tension in one direction did not give an effect similar to the one observed.

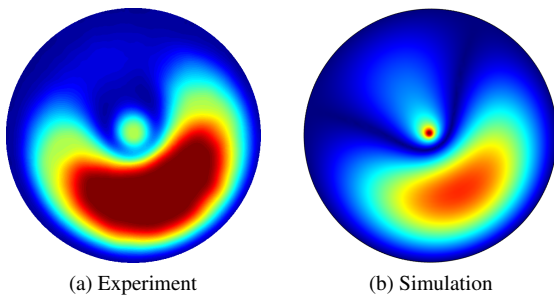


Figure 4: Highly asymmetrical operating deflection shape at 872 Hz and the simulated deformation at the same frequency.

Figure 5 shows asymmetry in the vibrational shapes of the cuica at high frequencies. Processed ESPI images are compared to corresponding operating deflection shapes calculated in COMSOL. Even without unwrapping, the main modes of vibration can be clearly seen in enhanced filtered images since the side lobe peak intensity decreases with rising deformation amplitude.

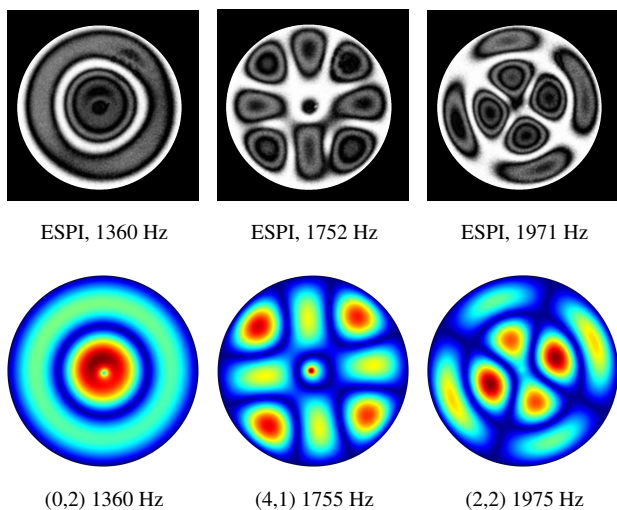


Figure 5: Slight asymmetry in the vibration shapes and corresponding FEM simulations. Top: temporally averaged and filtered ESPI images. Bottom: FEM simulations.

Such filtered ESPI images can be used for an initial modal analysis of vibrating structures and reveal vital information on

the operating deflection shapes of the object under study. The presented experimental setup requires only basic infrastructure in order to be restored. It is thus suitable for application across a range of scientific disciplines and research institutions.

#### 4.2. LDV verification

A single-point laser Doppler vibrometer was used in order to verify the obtained phase values. Table 2 shows a comparison between LDV results and unwrapped data at three single points chosen randomly on the surface of the membrane for two different frequencies. The average discrepancy is about 35 nm, which is in the order of  $\lambda/15$ .

Point	260 Hz		750Hz	
	ESPI, $\mu\text{m}$	LDV, $\mu\text{m}$	ESPI, $\mu\text{m}$	LDV, $\mu\text{m}$
1	0.074	0.08	0.29	0.25
2	0.176	0.2	0.17	0.2
3	0.1	0.09	0.26	0.28

Table 2: Comparison of the results of ESPI and LDV measurements for two frequencies at three different points on the membrane.

## 5. CONCLUSIONS

The vibration modes of a Brazilian cuica drum were investigated under harmonic excitation between 200 Hz and 2000 Hz by means of time-averaging ESPI followed by digital processing, which gave an adequate agreement with FEM modeling and LDV single-point results. The proposed filtering and processing algorithms give high-contrast ESPI images and competent quantitative data on absolute values of deformations due to external excitation. For several frequencies, the observed operating deflection shapes are similar to simple clamped membrane normal modes. However, non-symmetry of the cuica notably affects deformation shapes, which can be visualized on a computer screen in real time while changing frequency and excitation force.

Future work will involve the analysis of nonlinear behavior and transient events by means of high-speed ESPI in order to describe excitation processes in friction drums.

## 6. ACKNOWLEDGEMENTS

The authors would like to thank Alexander Mayer for technical assistance and development of data acquisition software in LabVIEW. This research work has been funded by the European Commission within the ITN Marie Curie Action project BATWOMAN under the 7th Framework Programme (EC grant agreement no. 605867).

## 7. REFERENCES

- [1] A. Akay, "Acoustics of friction," *The Journal of the Acoustical Society of America*, vol. 111, pp. 1525–1548, 2002.
- [2] P. Hariharan, *Basics of Interferometry*, Academic Press, 2007.
- [3] E. V. Jansson, "An investigation of a violin by laser speckle interferometry and acoustical measurements,"

*Quarterly Progress and Status Report*, vol. 13, no. 1, pp. 25–33, 1972.

- [4] T. D. Rossing, “Acoustics of percussion instruments: Recent progress.” *Acoustical Science and Technology*, vol. 22, pp. 177–188, 2001.
- [5] G. Bissinger and D. Oliver, “3-D Laser Vibrometry on Legendary Old Italian Violins,” *Sound and Vibration*, pp. 10–14, 2007.
- [6] R. Perrin, D. P. Elford, L. Chalmers, G.M. Swallowe, T. R. Moore, S. Hamdan, and B. J. Halkon, “Normal modes of a small gamelan gong,” *The Journal of the Acoustical Society of America*, vol. 136, no. 4, pp. 1942–1950, 2014.
- [7] R. Jones and C. Wykes, *Holographic and Speckle Interferometry*, Cambridge University Press, 2nd edition, 2001.
- [8] W. C. Wang, C. H. Hwang, and S. Y. Lin, “Vibration measurement by the time-averaged electronic speckle pattern interferometry methods.,” *Applied Optics*, vol. 35, no. 22, pp. 4502–4509, Aug. 1996.
- [9] J. Schneider, *Dictionary of African Borrowings in Brazilian Portuguese*, Buske Verlag, 1991.
- [10] C. Eduardo and F. Kumor, *Drum circle: A Guide to World Percussion*, Alfred Music Publishing, 2001.
- [11] T. R. Moore and J. J. Skubal, “Time-averaged electronic speckle pattern interferometry in the presence of ambient motion. Part I. Theory and experiments.,” *Applied optics*, vol. 47, no. 25, Sept. 2008.
- [12] J. W. Goodman, *Laser speckle and related phenomena*, Springer, 1975.
- [13] K. Creath, “Phase-shifting speckle interferometry,” *Applied Optics*, vol. 24, no. 18, 1985.
- [14] N. H. Fletcher and T. D. Rossing, *The physics of musical instruments*, Springer, 1998.
- [15] W. K. Schomburg, “Membranes,” in *Introduction to Microsystem Design*, vol. 1, pp. 29–52. 2011.
- [16] C. Li, C. Tang, H. Yan, L. Wang, and H. Zhang, “Localized Fourier transform filter for noise removal in electronic speckle pattern interferometry wrapped phase patterns.,” *Applied Optics*, vol. 50, no. 24, pp. 4903–11, Aug. 2011.